Available online at www.sciencedirect.com

ScienceDirect

Underground Space 4 (2019) 48–58

www.elsevier.com/locate/undsp

# Application of a finite element method to stress distribution in buried patch repaired polyethylene gas pipes

R. Khademi-Zahedi *, M. Shishesaz

*Shahid Chamran University of Ahvaz, Ahvaz, Iran*

Received 18 February 2018; received in revised form 15 April 2018; accepted 6 May 2018
Available online 6 July 2018

**Abstract**

Advantages of polyethylene pipes over traditional steel or metal pipes have increased industry interest in the use of polyethylene (PE) pipelines for underground applications and especially in gas distribution networks. In this study, finite element analysis is used to calculate the stress distribution in a patch repaired defective gas pipe under internal pressure. The pipe is assumed to be buried at a depth of 125 cm. The material is assumed to be medium density PE80B, where the patch material was selected from high density polyethylene (HDPE). During the loading process, the seasonal pipe temperature changes, surcharge loads, soil column weight, and soil–pipe interaction were included in the analysis. Four types of patch arrangements were selected to repair the damaged pipe. The shape of the defect hole was deemed as circular or elliptic. With respect to elliptic defects, various minor to major diameter ratios, $a/b$, were selected to simulate a circular to a crack shaped defect. Based on the results, the semi-circular and saddle fusion patches decrease the peak von Mises stress in the pipe by almost the same amount. However, the minimum peak von Mises stress in the patch corresponds to the saddle fusion repair arrangement. Based on the results, with respect to a saddle fusion repair, when the shape of the defect approaches a crack, the peak von Mises stress in the pipe almost doubles and exceeds the pipe allowable stress for a working life of 50 years. With respect to higher values of $a/b$, the stress level in the patch repaired pipe is significantly below its limiting value for the same life expectancy.


*Keywords:* Patch repair; Buried gas pipe; MDPE; HDPE; Temperature variation

## 1 Introduction

Today polymer materials are widely used in construction areas and especially in the pipeline industry. Polyethylene is a thermoplastic polymer that is composed of long chains of monomer ethylene. Polyethylene pipes and related fittings are widely adopted for water, sewage, and natural gas distribution networks in several countries. Additionally, industry interest in the use of PE pipes as an alternative to traditional steel or metal pipes remains high. Over a period of several years, PE pipes provide numerous benefits when compared to traditional steel or metal pipes. The aforementioned advantages include coilability, light weight, flexibility, high ductility, weldability, and reduced installation costs. Polyethylene material is resistant to corrosion, abrasion, and impact. The aforementioned advantages provide both performance and economic benefits that in turn lead to the popularity of polyethylene pipes in ploughing-in and trenchless technology applications.

In the recent 60 years, several advancements occurred in polyethylene production technology. This has led to different products including PE80, PE80B, PE80C, and PE100 materials that are currently used across the world. Specifically, PE80B and PE80C pipe materials are recognized as offering excellent long-term performance as pressure pipes. Medium density PE80B and high density PE100 materials

* Corresponding author.
*E-mail address:* reza.khademi.zahedi@gmail.com (R. Khademi-Zahedi).

https://doi.org/10.1016/j.undsp.2018.05.001

**Nomenclature**

| | |
|---|---|
| $A$ | difference between maximum and minimum temperatures for the time period in question (°C) |
| $C$ | design coefficient |
| $D_i$ | inner pipe diameter (mm) |
| $D_o$ | outer pipe diameter (mm) |
| $E'$ | embedment soil modulus (MPa) |
| $E_p$ | pipe elastic modulus (MPa) |
| $h$ | pipe thickness (mm) |
| $K_b$ | bedding factor |
| $l$ | pipe length in the model (mm) |
| $L_d$ | deflection lag factor |
| $F_{MRS}$ | maximum reduced strength (MPa) |
| $p_i$ | pipe inside pressure (MPa) |
| $P_T$ | total load above the pipe (MPa) |
| $D_{SDR}$ | standard dimension ratio ($D_{SDR} = \frac{D}{h}$) |
| $t$ | time (s) |
| $t_o$ | time for duration of a complete cycle (s) |
| $T(y, t)$ | induced temperature in the soil (°C) |
| $\overline{T}$ | average temperature for the time period in question (°C) |
| $W$ | combined weight of first two axels (N) |
| $y$ | depth of the pipe (cm or mm)) |
| $\alpha$ | thermal diffusivity of the soil ($cm^2$/sec) at penetration depth |
| $\alpha_t$ | pipe coefficient of thermal expansion 1/°C |
| $\Delta T$ | temperature change (°C) |
| $\Delta x$ | pipe horizontal deflection (mm) |
| $\upsilon$ | Poisson's ratio |
| $\sigma$ | normal stress in the pipe (MPa) |
| $\sigma_e$ | Von Mises stress (MPa) |
| $\sigma_{\theta\theta}$ | tangential stress in the pipe (MPa) |
| $\sigma_{rr}$ | radial stress in the pipe (MPa) |
| $\sigma_{zz}$ | longitudinal stress in the pipe (MPa) |

find immense utility in ploughing-in applications due to their flexibility and ease of coiling.

In summary, for a buried pipe, a supporting envelop is constructed by the surrounding soil with firm and stable materials. The envelop is often referred to as the "embedment". The amount of support by the embedment is directly proportional to its stiffness. Hence, often the embedment material is compacted (The Plastic Pipe Institute, 2006b, chap. 7). The stiffness of the materials placed above the pipe may also affect the pipe's performance. A significant load reduction on the pipe may occur due to the arching effect in the soil. This results in a complex stress distribution in the soil above and around the pipe. An increase in the stiffness of the backfill above the pipe increases the amount of arching that occurs.

The use of any pipe in conjunction with its mechanical properties and geometric design requires strict attention to minimize the stress level caused by the applied loads (The Plastic Pipe Institute, 2006b, chap. 7; Watkins & Anderson, 2000). The required information to investigate polyethylene pipes and fittings can be obtained via stress and strain analysis. The applied loads on a buried gas pipe must include daily and/or seasonal temperature changes, weight of the soil above the pipe, surcharge loads, inside pipe pressure, and stress concentration due to any local discontinuity or any external attachment to the pipe (Shishesaz, 2003, 2008). The resulting stress produced in a buried pipe due to the applied loads was first determined by Marston. Subsequently, Spangler used linear elasticity in conjunction with experimental studies to propose the Iowa formula. The formula predicts flexible buried pipe deflection under applied loads (Moser & Folkman, 2008, chap. 7). Watkins and Anderson (2000) developed a more advanced formula to calculate the elastic modulus of the soil around a buried pipe that yields better results when compared to Sprangler's formula.

With respect to a better estimation of the behavior of PE pipes under the applied loads, several authors (Goddard, 1994; Kolonko & Madryas, 1996) attempted to investigate the soil–pipe interaction effect of sewerage plastic pipes. The performance of elevated temperature on the buried high density polyethylene (HDPE) pipes was also investigated by Alawaji (2008). In his study, the effect of temperature on deformation characteristics and performance of HDPE was investigated. The testing program was composed of a ring pipe submerged in heated water at various temperatures. Popelar (1986) investigated the mechanical and creep properties of polyethylene gas pipe materials, namely PE23061X and PE3408IV. In the study, stress stain diagrams were obtained under different conditions. Teoh and Ong (1995) also investigated the pressure rupture in HDPE pipes.

In structural design process, it is necessary to properly design structures such that they perform safely during their life time expectancy. Thus, it is necessary for designers to possess a fundamental understanding of the behavior and failure of the material that is used (Budarapu & Rabczuk, 2017; Rabczuk, 2013; Rabczuk & Belytschko, 2006; Rabczuk & Eibl, 2006; Talebi, Silani, & Bordas, 2014; Talebi, Silani, & Rabczuk, 2015). Due to several reasons, polyethylene gas pipes can be damaged during long term use. This can result in the leakage of gas that must be prevented in the shortest possible time with minimum repair cost. Thus, different repair methods were developed and include patch repair (or saddle fusion) of the injured portion.

The method of electrofusion for joining two PE pipes was discussed by Mehrabi and Bowman (1997) while Green et al. (2006), Harris (2007) and Willie et al. (2006)

focus on the design tools and repairing methods applied to defective polyethylene gas pipes.

In the study conducted by Green et al. (2006) a remote external tool was developed to repair a defective PE gas pipe by using a polyethylene patch without introducing any interruption in gas flow inside the pipe. Harris (2007), examined the development of a patch composed of a solvent swollen polyethylene film that could be applied to a live natural gas line. The patch was applied under elevated temperature conditions allowing for a modified solvent weld and effectively repairing the pipe line in a quarter of the time required for repairing process. Experimental studies performed by Chua (1986) included the time dependence interaction of the soil and flexible pipes. Popelar, Popelar, and Kenner (1990) performed a comprehensive study to determine the mechanical behavior and properties of medium density polyethylene (MDPE) and HDPE that are commonly used in the gas pipe industry.

A heat fused MDPE or HDPE gas pipe is corrosion and chemical resistant and the pipe itself provides a maintenance free system with the exception of infrequent third party or any other type of damages. With respect to a damaged PE pipe, repair methods may be used to bring the pipe back into service as soon as possible or even repair the pipe without any interruption in gas flow. A principal method to achieve the goal involves the use of a saddle or a patch on the damaged portion of the pipe. This in turn introduces a local discontinuity in the gas line and may impose additional unwanted stress on the pipe.

Due to the complexity of the model, buried pipe simulations are computationally expensive and involve several minutes to hours of CPU usage. Improvements in the accuracy of the results without increasing the computational costs is of immense concern. Generally, the uncertainty in the model outputs increases as the models become increasingly complex. This is due to the randomness in the input parameters (Vu-Bac, Lahmer, & Zhuang, 2016). Therefore, uncertainties that could arise in the input parameters, such as internal pressure, temperature changes, surcharge load, soil column weight, defect geometry, and pipe and patch mechanical properties, should be carefully considered to determine the change in the model output (maximum von Mises stress) due to variation in the aforementioned inputs. Uncertainty and sensitivity analysis are very important for the aforementioned purposes (Hamdia, Silani, & Zhuang, 2017; Vu-Bac et al., 2016).

To the best of authors' knowledge, all previous studies that used finite element analysis (FEA) to investigate the soil-pipe interaction of the buried PE pipes did not focus on the effect of a local patch repair on stress distribution in overall behavior of the defective pipe. Thus, the purpose of the study is to investigate the effect of patch size and shapes and a saddle fusion repair on stress distribution that arises around the defective portion of the pipe. This can lead to a safe and solid field repair (when applicable) without any interruption in gas flow through the pipe.

## 2 Basic design theory

The design of underground gas pipes is based on the principle of soil–pipe interaction. Thus, the pipe and its surrounding soil act collectively to control the pipe performance. In the study, in order to incorporate the interaction and determine the effect a saddle fusion repair (or a patch fusion repair) on resulting stresses, the following thermal and mechanical loads (explained in Sections 2.1–2.3) are recognized and applied to the buried gas pipe for selected patch arrangements, namely, saddle, semi cylindrical, partial square, and circular patches.

### *2.1 Temperature variation in the soil*

Temperature variations in the soil (and thus in the pipe) might occur during a day or any seasonal changes may occur annually. Information on ground temperature is necessary to calculate the thermal stresses developed in the buried pipe. In the present study, the selected area was assumed as city of Ahvaz (south-west of Iran) in which the average ground or asphalt temperature in summer varies from 30 °C in the morning to approximately 67 °C in the early afternoon (Tabatabaii and Ameri, 1999). Similarly, on a cold winter day, the variation ranges from 0 °C in the morning to approximately 28 °C in the afternoon. Thus, at any depth, the ground temperature may be calculated based on Eq. (1) as follows:

$$T(y,t) = \bar{T} + A\exp\left[-y\left(\frac{\pi}{\alpha\, t_o}\right)^{\frac{1}{2}}\right] \times \cos\left[\frac{2\pi t}{t_o} - y\left(\frac{\pi}{\alpha t_o}\right)^{\frac{1}{2}}\right], \tag{1}$$

where $T(y, t)$ denotes the induced temperature in the soil, $y$ denotes the depth in question (cm), $t$ denotes the time (s), $\bar{T}$ denotes the average climate temperature for the time period and location of interest, $A$ denotes the difference between maximum and minimum temperatures for the time period and location of interest, $\alpha$ denotes the thermal diffusivity of the soil ($cm^2/s$) at the penetration depth and $t_o$ denotes the time for a complete temperature cycle. Although the results in the study are obtained for city of Ahvaz, they can be applied to any other location with similar seasonal changes in climate annually.

Based on TR-21/2001 (The Plastic Pipe Institute, 2001), in the absence of any other effects, the thermal stresses induced in PE pipes are calculated based on Eq. (2) as follows:

$$\sigma = E_p \cdot a_t \Delta T, \tag{2}$$

where $E_p$ denotes the pipe elastic modulus, $\alpha_t$ denotes the pipe coefficient of thermal expansion 1/°C, and $\Delta T$ is the pipe's temperature change within any specific period.

According to Eq. (1), on a hot summer day in city of Ahvaz, at a depth of approximately 120 cm, the soil temperature remains constant and equal to approximately 35 °C. However, on a cold winter day, at the same depth,

the equation predicts a constant ground temperature of 13 °C on a daily basis. Thus, on an annual basis, a buried patched pipe at a depth of 125 cm experiences a seasonal cyclic temperature change of 22 °C (Shishesaz, 2008).

### 2.2 Soil column weight above the pipe

The calculation of the dead load that is the permanent load from the weight of the soil as well as that of the pavement is extremely important in buried pipe design. In polyethylene pipe design, it is assumed that the overburden load applied to the pipe crown is equal to the weight of the soil column projected above the pipe. However, the actual load applied to a buried polyethylene gas pipe may indeed be significantly lower than that of the aforementioned load since the shear resistance transfers part of the soil load to the trench sidewalls and embedment. Theoretical approaches for calculating soil column weight load on the buried pipe crown are well described by Chevron Philips Chemical Company (2003, chap. 7).

### 2.3 Surcharge load in terms of traffic load on the pipe.

The pressure on the pipe due to a surface vehicular live load (mainly wheel loads from trucks and trains) depends on vehicle weight, tire pressure and size, vehicle speed, and several other factors. The most common loading used in design is the H20 highway loading. The wheel loading for H20 trucks is calculated based on the American Association of State Highway and Transportation Officials (AASHTO) standards. Wheel loading may be treated to act as a distributed or a concentrated load on the pavement. Shishesaz (2008) and Chevron Philips Chemical Company (2003, chap. 7) describe theoretical approaches for calculating vehicular live load on buried pipes.

In addition to the loads described in Sections 2.1–2.3, the inside gas pressure results in significant stresses in the pipe wall material. In the study, the operating inside pressure is assumed as equal to 4 bar. This is the working pressure in the metropolitan gas line in Iran. Additionally, it is possible to postulate the presence of stress concentration in the pipe due to a local discontinuity (or external attachments) that may arise from a major repair in the form of a saddle or patch fusion.

## 3 Gas pipe load calculations and models

### 3.1 Designing polyethylene gas pipes to withstand loads

The induced stresses in polyethylene gas pipes are due to a combination of internal and external loads. The most common internal force originate from the gas pressure. Conversely, in buried gas pipes, the most common external loads are the earth and surcharge loads and the thermal and soil–pipe interactions.

There are a few methods to calculate PE pipe stresses. Essentially, polyethylene pipes are viscoelastic in nature. Thus, as the first method, the effect is included in the modeling process in any stress calculation. Another method that is vastly used by several designers involves treating PE as a linear elastic material and comparing the resulting stresses with the minimum required strength (MRS) that account for the reduction in strength of polyethylene due to its viscoelastic nature in time (at any specific temperature). Table 1 shows the MRS values of PE100 and PE80B for a life expectancy of 50 years.

Based on ISO Standard 12162 (2004), or EN 1555-1 (1996), with respect to thermoplastic pipe materials, the design stress (or maximum allowable stress that can be applied to the pipe) at 20 °C and 50 years of life expectancy is as follows:

$$\sigma_s = \frac{F_{MRS}}{C}, \tag{3}$$

Here, $\sigma_s$ denotes the design stress, $F_{MRS}$ corresponds to the minimum required strength, and $C$ denotes the design coefficient (at least 1.25 for all PE types). Based on the latter standard that is widely used by Iranian gas companies, the maximum operating pressure ($P_{max}$) is calculated as follows:

$$P_{max} = \frac{20 \times F_{MRS}}{C(D_{SDR} - 1)}, \tag{4}$$

In Eq. (4), $D_{SDR}$ denotes the standard dimension ratio. This is the ratio of the outside diameter to the wall thickness of the pipe. In addition to any numerical solution, a method to calculate the plastic pipe deflection denotes the use of Sprangler's Modified Iowa Formula (Chevron Philips Chemical Company, 2003, chap. 7) that is expressed as follows:

$$\frac{\Delta x}{D_i} = \frac{P_T}{144}\left(\frac{K_b L_d}{\frac{2E_p}{3}\left(\frac{1}{D_{SDR}-1}\right)^3 + 0.061E'}\right) \tag{5}$$

Here, $\Delta x$ denotes the horizontal deflection of the pipe, $K_b$ denotes the bedding factor (typically, 0.1), $L_d$ denotes the deflection lag factor, $E_p$ denotes the pipe diameter, $E'$ denotes the embedment soil modulus, and $D_i$ denotes the inner diameter of the pipe. Evidently, in the aforementioned pipes, the percent deflection is as follows:

$$\text{Deflection} = \frac{\Delta x}{D_i} \times 100\% \tag{6}$$

Table 1
MRS values of PE80B and PE100 for a life period of 50 years (Shishesaz, 2008).

| PE80B (MPa) | PE100 (MPa) | Working period (years) | Working temperature (°C) |
|---|---|---|---|
| 8.0 | 10.0 | 50 | 20 |
| 7.5 | 9.4 | 50 | 25 |
| 7.0 | 8.7 | 50 | 30 |
| 6.4 | 8.0 | 50 | 35 |
| 6.0 | 7.3 | 50 | 40 |

Based on Chevron Philips Chemical Company (2003, chap. 7), in order the results to be valid based on the elastic assumption for the pipe material, the maximum allowable percent deflection for the flexible pipes with $D_{SDR} = 11$ is $\leqslant 3\%$.

As shown in Fig. 1, for unburied large cylindrical pipes with a small circular hole, the maximum hoop, radial, and longitudinal stresses are expressed as follows (Khademi-Zahedi, 2011):

$$(\sigma_{\theta\theta}) = \frac{P_i(4k^2 + 2 - 2\upsilon)}{(k^2 - 1)} \tag{7}$$

$$\sigma_{rr} = -P_i\ , \quad \sigma_{zz} = \frac{2\upsilon P_i}{(k^2 - 1)} \tag{8}$$

In Eqs. (7) and (8), $k = D_o/D_i$ (where $D_i$ and $D_o$ denote the inner and outer pipe diameters, respectively), $\upsilon$ denotes the Poisson's ratio ($\upsilon = 0.35$ for MDPE), and $P_i$ denotes the inside pipe pressure. Thus, using von Mises stress $\sigma_e$ as the maximum allowable stress before pipe failure, the following expression is obtained with respect to MDPE pipes (Khademi Zahedi et al., 2018):

$$\sigma_e = \frac{P_i\left[21k^4 + 3.6k^2 + 0.27\right]^{1/2}}{(k^2 - 1)} \tag{9}$$

Due to the complex nature of the repaired pipe geometry and soil-pipe interaction, it is customary to use finite element method (FEM) to solve for the stress distribution within the pipe and its attachments. Several authors (Areias & Rabczuk, 2013; Chau-Dinh, Zi, & Lee, 2012; Nguyen-Thanh, Kiendl, & Nguyen-Xuan, 2011; Rabczuk, Areias, & Belytschko, 2007; Rabczuk, Zi, & Bordas, 2010) used numerical and other alternative methods (Amiri, Anitescu, & Arroyo, 2014; Amiri, Milan, & Shen, 2014; Areias, Rabczuk & Msekh, 2016; Nguyen-Thanh et al., 2015; Khademi Zahedi et al., 2018) to solve for stress distribution in shell structures. Additionally, damage and fracture algorithms for the computer implementation of fracture using different discretization and meshing techniques were presented in Amiri, Anitescu, et al. (2014), Amiri, Milan, et al. (2014), Areias, Rabczuk, and Dias-Da-Costa (2013), Areias, Rabczuk, and Camanho (2014), Areias, Msekh, et al. (2016), Areias, Rabczuk, et al. (2016), Areias and Rabczuk (2017), Budarapu, Gracie, and Bordas (2014), Budarapu, Gracie, and Yang (2014), Rabczuk, Bordas, et al. (2010), and Rabczuk, Gracie, et al. (2010). Furthermore, contributions on isogeometric analysis to analyze shell structures can be found in Ghasemi et al. (2017), Ghorashi et al. (2015), Nguyen-Thanh, Zhou, and Zhuang (2017), Vu-Bc et al. (2018).

### 3.2 Buried pipe model

In order to investigate the stress distribution in a pressurized PE gas pipe, a pipe with an outer diameter of 114.3 mm was selected with $D_{SDR} = 11.5$. Based on the selected pipe diameter, the thickness was calculated based on the $D_{SDR}$ value. The damaged buried pipe was then modeled based on various patch shapes as shown in Fig. 2.

The trench dimensions and pipe surrounding were selected based on Fig. 3(a). As mentioned previously in Section 2.3, the most common traffic load used in pipe design is the H20 highway loading. Based on AASHTO standards, the wheel loading for H20 trucks is calculated based on Fig. 3(b). Furthermore, the pipe itself is surrounded by different layers of soil in which the properties of each layer are listed in Table 2. As stated previously,

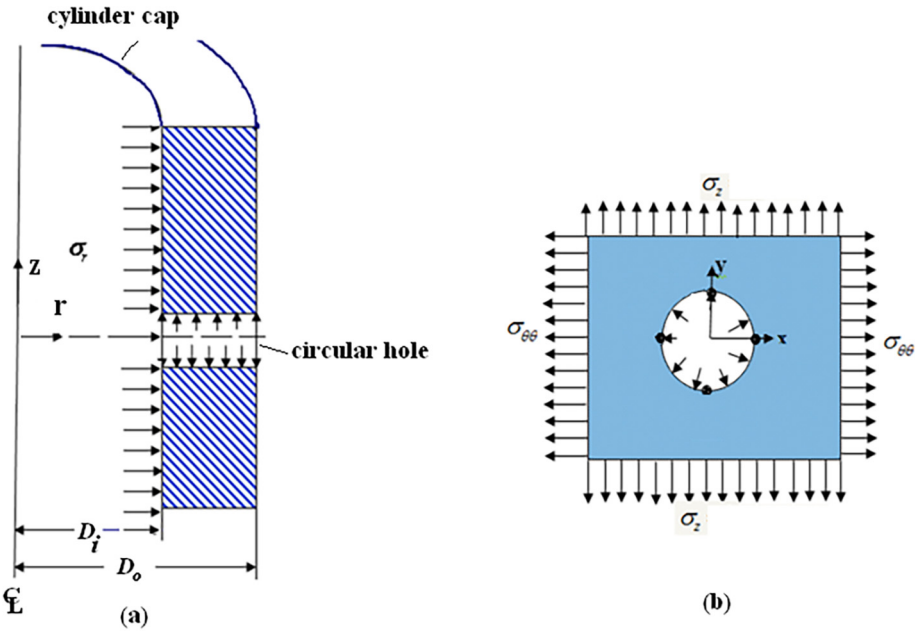


Fig. 1. (a) Cylinder or large size pipe under internal pressure; (b) hoop and axial stress distribution on a portion of the cylinder or pipe in the $x$–$y$ plane.

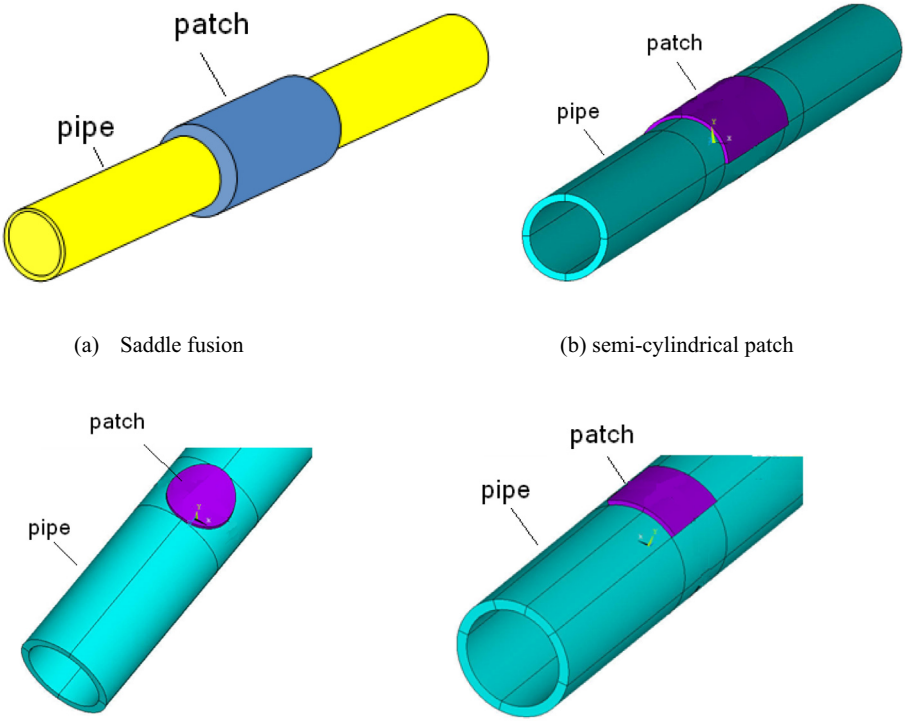


(a) Saddle fusion (b) semi-cylindrical patch

(c) circular partial patch (d) Square partial patch

Fig. 2. Various shapes of patches used to repair the damaged pipe in in finite element models.

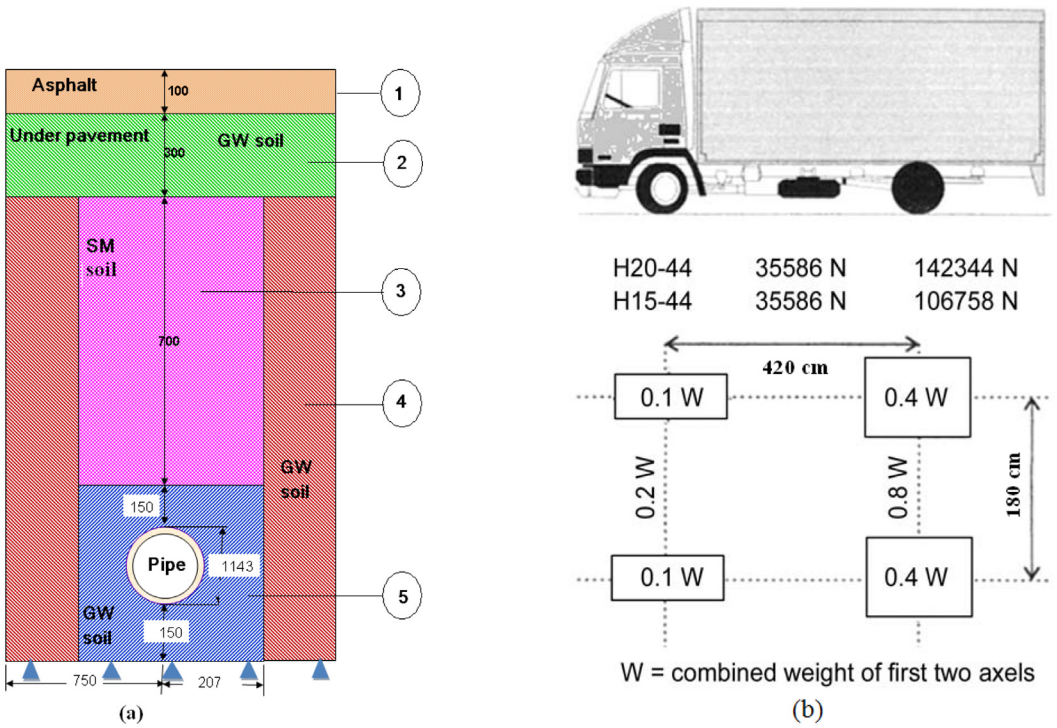


Fig. 3. (a) Trench dimensions and pipe surrounding in mm (for description of soil layers ① to ⑤ see Table 2); (b) traffic loading [3].

polyethylene material undergoes creep in the long term, and thus it is customary in design to use a reduced strength based on a 50 years life time and treat the material as linear elastic in calculations (Chevron Philips Chemical Company, 2003, chap. 7; Khademi Zahedi et al., 2018; The Plastic Pipe Institute, 2006a, chap. 6). The magnitude

Table 2
Properties of each soil level around and above the pipe (see Fig. 3(a)).

| Layer No. | Type of the soil | Modulus of elasticity (MPa) | Density (kg/m$^3$) | Poisson's ratio |
|---|---|---|---|---|
| 1 | Asphalt | 173.0 | 2 200 | 0.35 |
| 2 | GW soil with 90% Proctor density | 6.9 | 1 700 | 0.20 |
| 3 | SM soil with 90% Proctor density | 6.9 | 1 900 | 0.35 |
| 4 | GW soil with 95% Proctor density | 15.0 | 2 000 | 0.35 |
| 5 | GW soil with 85% Proctor density | 4.8 | 1 600 | 0.20 |

of the traffic load due to H20 truck loading was selected as 544 780 Pa. This accounted for any dynamic load exerted on the pipe by the wheels. Additionally, as stated previously, the inside pipe pressure was assumed as equal to 4 bar (405 300 Pa). This is the actual pressure that used in domestic gas pipelines in the metropolitan area of Iran.

### 3.3 Finite element model of the patch repaired gas pipe

Soil grades around the pipe's circumference were selected based on ASTM standards. With reference to Eq. (1) based on Fig. 3(b), a burial depth of 125 cm was selected for the pipe. At this depth, on a daily basis, any climate changes at the ground level do not appear to affect the pipe temperature (Shishesaz, 2008). The pipe was assumed as buried in a trench with a width of 414 mm while surrounded by a layer of fine gravel. The ground surface was assumed as covered by a thick layer of asphalt. The effect of traffic load in terms of distributed or concentrated loads on the pipe was also included. The ANSYS V12 finite element code was used for modeling and analysis of the pipe and its surrounding. The element used to model the pipe, patch, and the surrounding medium was solid95. This is a twenty-node element designed for structural purposes in which each node exhibits three degrees of freedom (three translations in $x$, $y$, and $z$ directions). The soil–pipe interaction was also incorporated in the model by using face to face contact elements (contacta 172 and target 170). The length of the patch (Figs. 2(a), (b), and (d)) or its diameter (Fig. 2(c)) was assumed as 76 mm. Fig. 4(a) shows the FE model of a half of the pipe in its surrounding medium. A magnified view of the pressurized pipe (with a patch on its defective area) is shown in Fig. 4(b). The pipe material was selected from PE80 while PE100 was used for the patch. Furthermore, the effect of the traffic load, soil weight, temperature change of the pipe, inside pressure, and the presence of patch on the defective area were all included to investigate their overall effect on stress distribution in the repaired PE pipe. A fine mesh was applied to regions near the defective area while it was allowed to become coarser in areas far from the defect. In order to obtain accurate results, the postulated model was executed based on different mesh conditions (and element numbers) until adequate convergence was reached.

### 3.4 Methodology to globalize the study

In the study, the applicability of HDPE patch for repairing the defective buried MDPE gas pipe was investigated. Any variation in the soil temperature is necessary to calculate thermal stresses in the buried pipes, and thus Eq. (1) was used to determine any seasonal changes that may occur in the soil at any depth in question. Based on Eq. (1), on a daily basis, at different depths at approximately 125 cm, the ground temperature is nearly constant (Shishesaz, 2008). This implies that increases in the pipe installation depth to any logical value causes the pipe (or repaired pipe and its surrounding medium) to become insensitive to any changes in temperature during the daytime at ground level. Additionally, polyethylene possesses a high value of the coefficient of thermal expansion when compared to metals, and thus any temperature decrease in the pipe exhibits a

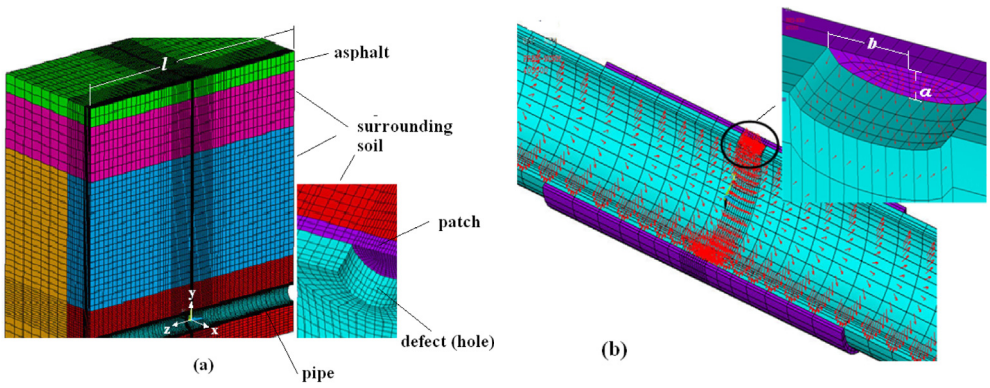


Fig. 4. (a) Finite element model of the patched pipe with surrounding soil; (b) pressurized pipe with an elliptical defect (surrounding soil is removed).

direct and a meaningful effect on thermal stresses developed in the pipe. Thus, the aforementioned results can also be applied to other regions with similar or smaller changes in climate temperature (annually) provided that other factors do not exceed the values used in the study.

## 4 Results and discussions

In order to verify the applicability of finite element method (FEM) for solution of such problems, the unburied pipe was modeled and loaded to a final pressure of 405 300 Pa (4 bar) while subjected to holes of various sizes as listed in Table 3. The value of $k$ was selected as equal to 1.21. The values of hoop and von Mises stresses obtained through finite element analysis and those in Eqs. (7) and (9) are reported in the table. As shown in the table, the percentage differences between finite element results and those obtained through Eqs. (7) and (9) are low. The aforementioned differences appear as a function of hole size and pipe diameter. Additionally, the applicability of FEM for stress distribution in buried PE pipes was verified in (Shishesaz, 2008).

In order to further investigate the effect of inside pressure and temperature change, traffic load, and the soil weight on the buried pipe with respect to stress concentration stemming from the patch, the finite element model of the repaired pipe and its surrounding area at a depth of 125 cm was considered. This is shown in Fig. 3(a). The traffic load imposed on the pavement was calculated based on Fig. 3(b). The hole in the pipe was assumed as repaired by four different types of patches as shown in Fig. 2. It was assumed that the pipe undergoes a maximum temperature decrease of 22 °C (due to a seasonal change in temperature). As stated previously, this is a typical seasonal temperature change in the soil at a depth of 125 cm in the city of Ahvaz that is located in a hot climate zone.

Based on finite element findings, the maximum horizontal deflection in the pipe for all selected circular defect sizes of 5, 7.5, 10, 12.5, 15, 17.5, and 20 mm (in diameter) was equal to 0.47 mm. The pipe diameters were considered as 101.6 mm (4 in.). Based on Eq. (6), this yields a percent deflection of 0.46% that is significantly below the 3% limit.

Figure 5 shows the variations in the maximum von Mises stress in the buried pipe for various size circular defects (holes). The strength of the pipe based on a 50 years working life is also superimposed. The reduced strength is used due to the viscoelastic behavior of polyethylene that occurs over the years of service. Based on the figure, the maximum von Mises stress that occurs in the unpatched defective pipe is significantly above the strength limit of the pipe at 35 °C for a working period of 50 years. With respect to the saddle fusion repaired pipe, in presence of all mechanical and thermal loads as previously expressed, the maximum von Mises stress decreases to a safe value such that the pipe withstands the inside pressure of 4 bar (405 300 Pa).

Figure 6 shows a similar behavior for a HDPE saddle fusion patch at various circular defect sizes and temperature changes. It is observed that the maximum von Mises stress based on a temperature decrease of 22 °C is significantly below the admissible stress for a life expectancy of 50 years. Based on the figure, increases in the defect diameter leads to a gradual increase in the peak von Mises stress in the patch.

Figures 7 and 8 show the effect of various patch shapes on Maximum von Mises stress for a seasonal temperature decrease of 22 °C in presence of other mechanical loads. Based on Fig. 7, the use of semi-circular and saddle fusion patches reduce the peak von Mises stress in the pipe by almost the same amount. However, based on Fig. 8, the minimum peak von Mises stress in the patch corresponds to the saddle fusion repair arrangement. Thus, with respect to the stress viewpoint, a saddle fusion patch appears safer for the repair of circular defects in buried pipes.

The effect of elliptical shaped holes with the major diameter located along length of the pipe is shown in Figs. 9 and 10. The ratio of a smaller to larger hole diameter, $a/b$, was

Table 3
Comparison of hoop and von Mises stresses obtained through FE solution and those from Eqs. (7) and (9) due to an inside pressure only.

| Hole diameter (mm) | Model length $l$ (m) (see Fig. 4(a)) | No. of elements in FE model | Maximum hoop stress (MPa) | | Difference (%) | Maximum von Mises stress (MPa) | | Difference (%) |
|---|---|---|---|---|---|---|---|---|
| | | | FEM | Eq. (7) | | FEM | Eq. (9) | |
| 5 | 0.5 | 10 395 | 5.82 | 6.25 | 6.9 | 5.70 | 6.02 | 5.32 |
| | | 13 346 | 5.82 | 6.25 | 6.9 | 5.71 | 6.02 | 5.15 |
| | 1.5 | 14 715 | 5.82 | 6.25 | 6.9 | 5.70 | 6.02 | 5.32 |
| | | 30 517 | 5.81 | 6.25 | 7.0 | 5.72 | 6.02 | 4.98 |
| 7.5 | 0.5 | 10 395 | 6.01 | 6.25 | 3.8 | 6.10 | 6.02 | 1.33 |
| | | 13 346 | 6.02 | 6.25 | 3.7 | 6.11 | 6.02 | 1.49 |
| | 1.5 | 14 715 | 6.02 | 6.25 | 3.7 | 6.11 | 6.02 | 1.49 |
| | | 30 517 | 6.03 | 6.25 | 3.5 | 6.13 | 6.02 | 1.83 |
| 10 | 0.5 | 10 395 | 6.44 | 6.25 | 3.0 | 6.46 | 6.02 | 7.31 |
| | | 12 399 | 6.43 | 6.25 | 2.9 | 6.47 | 6.02 | 7.47 |
| | 1.5 | 16 394 | 6.42 | 6.25 | 2.7 | 6.45 | 6.02 | 7.14 |
| | | 32 400 | 6.43 | 6.25 | 2.9 | 6.47 | 6.02 | 7.47 |

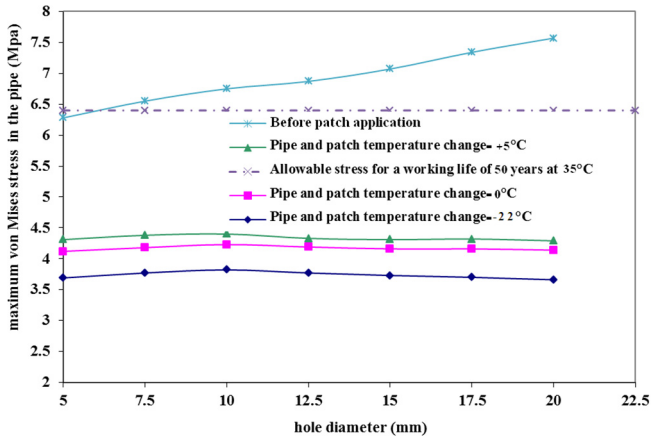


Fig. 5. Maximum von Mises stress in the buried pipe for various size circular hole defects.

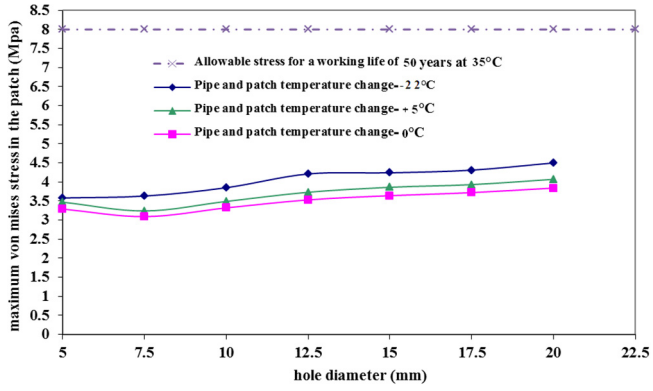


Fig. 6. Maximum von Mises stress in the saddle fusion patch for various size circular hole defects.

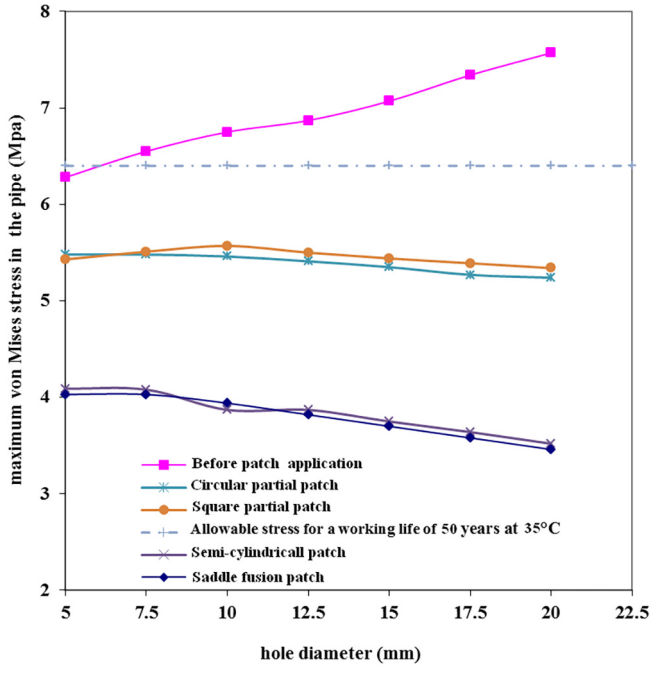


Fig. 7. Maximum von Mises stress in the pipe versus defect size (diameter) for various patch shapes, based on a seasonal temperature drop of 22 °C and other mechanical loads.

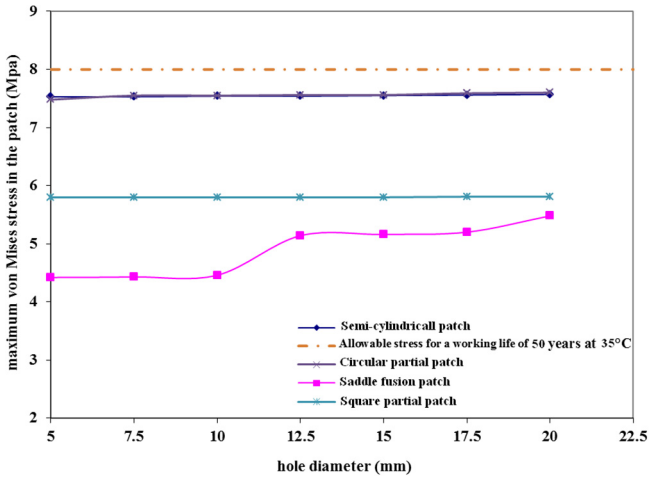


Fig. 8. Maximum von Mises stress in the patch versus defect size (diameter) for various patch shapes based on a seasonal temperature drop of 22 °C and other mechanical loads.

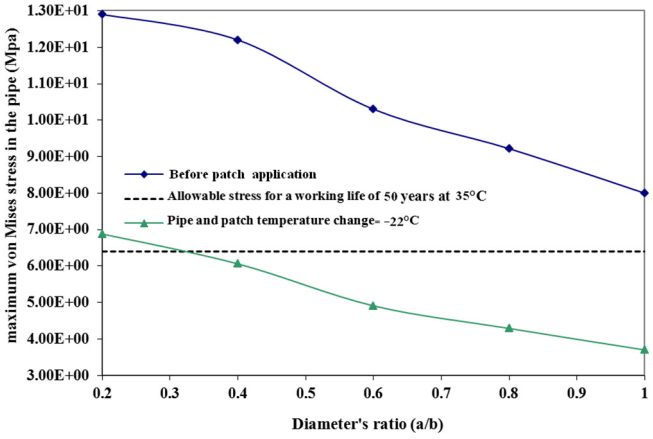


Fig. 9. Maximum von Mises stress in the pipe as a function of *a*/*b* ratio for saddle fusion patch.

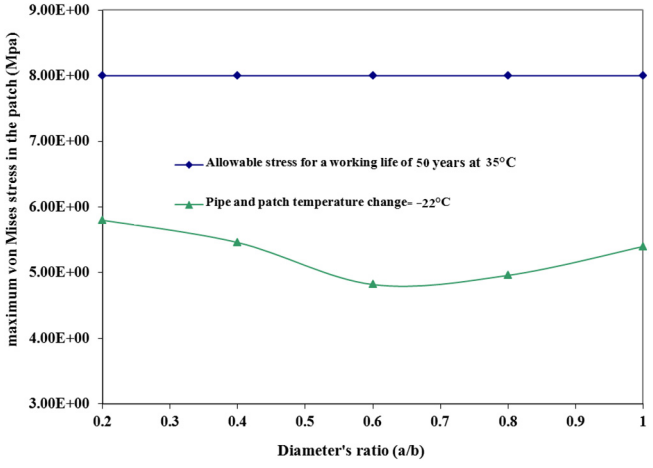


Fig. 10. Maximum von Mises stress in the patch as a function of a/b ratio for saddle fusion patch.

allowed to approach a low value to simulate almost a longitudinal crack along the pipe length (see Fig. 4(b)). Figure 9 shows the peak von Mises stress developed in the pipe as function of $a/b$ ratio for various patch shapes at a temperature decrease of 22 °C. In Fig. 10, similar results are plotted in the patch. In both the figures, the inside pressure is assumed as 4 bar, and the pipe was buried at a depth of 125 cm while subjected to the H20 loading condition. Based on Fig. 9, in a saddle fusion repair, when the defect shape approaches that of a crack, the peak von Mises stress in the pipe almost doubles and exceeds the allowable stress for a working life of 50 years. With respect to higher values of $a/b$, the stress level in the patch repaired pipe is significantly below its limiting value for the indicated 50 years life expectancy. Additionally, based on Fig. 10, in presence of all mechanical and thermal loads, for all ratios of $a/b$, the peak von Mises stress in the patch is significantly below its the allowable strength value for 50 years life time.

## 5 Conclusions

In the study, the finite element method is used to survey the effect of patch repair on stress distribution in a buried PE gas pipe at a depth of 125 cm. The postulated model is subjected to surcharge load, temperature change, soil column weight, and soil-pipe interaction, and an inside pressure of 4 bar. Four types of patch arrangements are selected to repair the damaged pipe and include circular, square, semi cylindrical, and saddle shaped patches. Based on the results, the semi-circular and saddle fusion patches reduce the peak von Mises stress in the pipe by almost the same amount. However, the peak von Mises stress in the patches appears as the least for the saddle fusion repair arrangement. Thus, under the proposed loading conditions, it is advisable to use this type of repair for defected gas pipes. Furthermore, with respect to elliptical defects with major axis along the pipe length, for $a/b$ ratios exceeding 0.32, the peak von Mises stress in the pipe remains below its allowable stress value for a working life of fifty year. With respect to all selected values of $\frac{a}{b}(0.2 \leqslant \frac{a}{b} \leqslant 1.0)$, the stress level in the patch appears significantly below its limiting value for the aforementioned life expectancy. With respect to elliptical defects repaired by a saddle fusion patch arrangement, the minimum value of peak von Mises stress in the patch appears to occur at $\frac{a}{b} \simeq 0.6$. Additionally, polyethylene exhibits a high value of coefficient of thermal expansion when compared to metals, and thus temperature decrease in the pipe exhibits a direct and significant effect on thermal stresses produced in the pipe. Thus, the aforementioned results can also be applied to other regions with lower changes in seasonal climate temperatures.

## References


Alawaji, H. A. (2008). Temperature effects on polyethylene (HDPE) and fiberglass (GRP) pipes. <http://www.ksu.edu.sa/sites/Colleges/Engineering/final Report/CE-23-26-27.pdf>.

Amiri, F., Anitescu, C., Arroyo, M., Bordas, S. P. A., & Rabczuk, T. (2014). XLME interpolants, a seamless bridge between XFEM and enriched meshless methods. *Computational Mechanics, 53*(1), 45–57.

Amiri, F., Milan, D., Shen, Y., Rabczuk, T., & Arroyo, M. (2014). Phase-field modeling of fracture in linear thin shells. *Theoretical and Applied Fracture Mechanics, 69*(2), 102–109.

Areias, P., Msekh, M. A., & Rabczuk, T. (2016). Damage and fracture algorithm using the screened poisson equation and local remeshing. *Engineering Fracture Mechanics, 158*, 116–143.

Areias, P., & Rabczuk, T. (2013). Finite strain fracture of plates and shells with configurational forces and edge rotation. *International Journal for Numerical Methods in Engineering, 94*(12), 1099–1122.

Areias, P., & Rabczuk, T. (2017). Steiner-point free edge cutting of tetrahedral meshes with applications in fracture. *Finite Element in Analysis and Design, 132*, 27–41.

Areias, P., Rabczuk, T., & Camanho, P. P. (2014). Finite strain fracture of 2D problems with injected anisotropic softening elements. *Theoretical and Applied Fracture Mechanics, 72*, 50–63.

Areias, P., Rabczuk, T., & Dias-Da-Costa, D. (2013). Element-wise fracture algorithm based on rotation of edges. *Engineering Fracture Mechanics, 110*(3), 113–137.

Areias, P., Rabczuk, T., & Msekh, M. (2016). Phase-field analysis of finite-strain plates and shells including element subdivision. *Computer Methods in Applied Mechanics and Engineering, 312*(C), 322–350.

Budarapu, P. R., Gracie, R., Bordas, S. P. A., & Rabczuk, T. (2014). An adaptive multiscale method for quasi-static crack growth. *Computational Mechanics, 53*(6), 1129–1148.

Budarapu, P. R., Gracie, R., Yang, S. W., Zhuang, X., & Rabczuk, T. (2014). Efficient coarse graining in multiscale modeling of fracture. *Theoretical and Applied Fracture Mechanics, 69*(2), 126–143.

Budarapu, P. R., & Rabczuk, T. (2017). Multiscale methods for fracture: A review. *Journal of the Indian Institute of Science, 97*(3), 339–376.

Chevron Philips Chemical Company LP (2003). Buried pipe design. *Bull, PP900, Book 2*, 81–115.

Chau-Dinh, T., Zi, G., Lee, P. S., Song, J. H., & Rabczuk, T. (2012). Phantom-node method for shell models with arbitrary cracks. *Computers & Structures, 92*(3), 242–256.

Chua, K. M. (1986). *Time-dependence interaction of soil and flexible pipe* (Ph.D. Thesis). Texas: Texas A&M University.

European Committee for Standardization (1996). EN 1555 – 1. Plastic piping systems for the supply of gaseous fuels – Polyethylene (PE) – Part 1: General.

Ghasemi, H., Park, H. S., & Rabczuk, T. (2017). A level-set based IGA formulation for topology optimization of flexoelectric materials. *Computer Methods in Applied Mechanics and Engineering, 313*, 239–258.

Ghorashi, S., Valizadeh, N., Mohammadi, S., & Rabczuk, T. (2015). T-spline based XIGA for fracture analysis of orthotropic media. *Computers and Structures, 147*, 138–146.

Goddard, J. B. (1994). Plastic pipe design. Columbus, Ohio, ADS. Technical note 4.103, pp. 1–30.

Green, K. H., Rochefort, W. E., Wannenmacher, N., Clark, J. A., & Harris, K. (2006). *Development of a remote external repair tool for damaged or defective polyethylene pipe. Technical report.* USA: Department of Chemical Engineering, Organ State University, Contract/Grant no. DE-FC26-03NT41879.

Hamdia, K., Zhuang, X., Silani, M., He, P., & Rabczuk, T. (2017). Stochastic analysis of the fracture toughness of polymeric nanoparticle composites using polynomial chaos expansions. *International Journal of Fracture, 206*(2), 215–227.

Harris, K. E. (2007). *Squeeze off and gel patch repair methods for polyethylene pipe in natural gass distribution lines* (M.S. Thesis). USA Oregon: Oregon State University.

International Organization For Standardization (2004). ISO 12162, Thermoplastics materials for pipes and fittings for pressure applications-Classification and designation-Overall Service (design) coefficient.

Khademi-Zahedi, R. (2011). *Stress distribution in patch repaired polyethylene gas pipes* (M.S. Thesis). Iran: Shahid Chamran University.

Khademi Zahedi, R., Alimouri, P., Nguyen-Xuan, H., & Rabczuk, T. (2018). Crack detection in a beam on elastic foundation using differential quadrature method and the Bees algorithm optimization. *Proceedings of the International Conference on Advances in Computational Mechanics*, 439–460. https://doi.org/10.1007/978-981-10-7149-2_30.

Kolonko, A., & Madryas, C. (1996). Modernization of underground pipes in towns in Poland. *Tunnelling & Underground Space Technology, 11*(2), 215–220.

Mehrabi, H. A., & Bowman, J. (1997). Electrofusion welding of cross-linked polyethylene pipes. *Iranian Polymer Journal, 6*(7), 195–203.

Moser, A. P., & Folkman, S. (2008). *Buried pipe design* (3rd ed.. USA: McGraw Hill Book Company (pp. 387).

Nguyen-Thanh, N., Kiendl, J., Nguyen-Xuan, H., Wüchner, R., Bletzinger, K. U., Bazilevs, Y., & Rabczuk, T. (2011). Rotation free isogeometric thin shell analysis using PHT-splines. *Computer Methods in Applied Mechanics and Engineering, 200*(47), 3410–3424.

Nguyen-Thanh, N., Valizadeh, N., Nguyen, M. N., Nguyen-Xuan, H., Zhuang, X., Areias, P., ... Rabczuk, T. (2015). An extended isogeometric thin shell analysis based on Kirchhoff-Love theory. *Computer Methods in Applied Mechanics and Engineering, 284*, 265–291.

Nguyen-Thanh, N., Zhou, K., Zhuang, X., Areias, P., Nguyen-Xuan, H., Bazilevs, Y., & Rabczuk, T. (2017). Isogeometric analysis of large-deformation thin shells using RHT-splines for multiple-patch coupling. *Computer Methods in Applied Mechanics and Engineering, 316*, 1157–1178.

Popelar, C. F. (1986). *Characterization of mechanical properties for polyethylene gas pipe materials* (M.S. Thesis). Ohio: The Ohio: State University.

Popelar, C. F., Popelar, C. H., & Kenner, V. H. (1990). Viscoelastic material characteristics and modeling for polyethylene. *Polymer Engineering and Science, 30*(10), 577–586.

Rabczuk, T. (2013). Computational methods for fracture in brittle and quasi-brittle solids: State-of-the-art review and future perspectives. *ISRN Applied Mathematics, 2013*(2013), 332–369.

Rabczuk, T., Areias, P. M. A., & Belytschko, T. (2007). A meshfree thin shell method for non-linear dynamic fracture. *International Journal for Numerical Methods in Engineering, 72*(5), 524–548.

Rabczuk, T., & Belytschko, T. (2006). Application of particle methods to static fracture of reinforced concrete structures. *International Journal of Fracture, 137*(1–4), 19–49.

Rabczuk, T., Bordas, S. P. A., & Zi, G. (2010). On three-dimensional modelling of crack growth using partition of unity methods. *Computers and Structures, 88*(23–24), 1391–1411.

Rabczuk, T., & Eibl, J. (2006). Modeling dynamic failure of concrete with meshfree particle methods. *International Journal of Impact Engineering, 32*(11), 1878–1897.

Rabczuk, T., Gracie, R., Song, J. H., & Belytschko, T. (2010). Immersed particle method for fluid-structure interaction. *International Journal for Numerical Methods in Engineering, 81*(1), 48–71.

Rabczuk, T., Zi, G., Bordas, S. P. A., & Nguyen-Xuan, H. (2010). A simple and robust three-dimensional cracking-practice method with enrichment. *Computer Methods in Applied Mechanics and Engineering, 199*(37–40), 2437–2455.

Shishesaz, M. R. (2003). Determination of design parameters in large size reinforced polyethylene pipes. *Iranian Polymer Journal, 12*(2), 109–114.

Shishesaz, M. R. (2008). Applicability of medium density polyethylene gas pipes in hot climate areas of south-west Iran. *Iranian Polymer Jornal, 17*(7), 503–517.

Tabatabaii, A., Ameri, M., & Behbahani, H. (1999). (1378) Prediction of asphalt cover temperature in city of Ahvaz (Iran). Journal of Engineering, Tabriz University, College of Engineering, 22 (Spring-summer Issue) (in Persian).

Talebi, H., Silani, M., Bordas, S., Kerfriden, P., & Rabczuk, T. (2014). A computational library for multiscale modelling of material failure. *Computational Mechanics, 53*(5), 1047–1071.

Talebi, H., Silani, M., & Rabczuk, T. (2015). Concurrent multiscale modelling of three dimensional crack and dislocation propagation. *Advances in Engineering Software, 80*, 82–92.

The Plastic Pipe Institute (2001). Thermal expansion and contraction in plastics piping systems, TR- 21/2001. <www.plasticpipe.org>.

The Plastic Pipe Institute (2006). Handbook of polyethylene pipe. Washington DC, pp. 157–260.

The Plastic Pipe Institute (2006). Handbook of polyethylene pipe. Washington DC, pp. 261–303.

Teoh, S. H., & Ong, E. H. (1995). Tensile and pressure rupture behavior of flow-formed high density polyethylene pipes. *Polymer, 36*(1), 101–107.

Vu-Bc, N., Duong, T. X., Lahmer, T., Zhuang, X., Sauer, R. A., Park, H. S., & Rabczuk, T. (2018). A NURBS-based inverse analysis for reconstruction of nonlinear deformations of thin shell structures. *Computer Methods in Applied Mechanics and Engineering, 331*, 427–455.

Vu-Bac, N., Lahmer, T., Zhuang, X., Nguyen-Thoi, T., & Rabczuk, T. (2016). A software framework for probabilistic sensitivity analysis for computationally expensive models. *Advances in Engineering Software, 100*, 19–31.

Watkins, R. K., & Anderson, L. R. (2000). *Structural mechanics of buried pipes*. New York: CRC Press (pp. 22–57).

Willie, E., Rochefort, W. E., & Green, H. (2006). Polyethylene pipe patching systems and methods. U.S. patent application 186256, filed 2006-01-31.